Molecular Cancer Therapeutics

Notch Inhibitor PF-03084014 Inhibits Hepatocellular Carcinoma Growth and Metastasis via Suppression of Cancer Stemness due to Reduced Activation of Notch1–Stat3

Chuan Xing Wu[1], Aimin Xu[2], Cathy C. Zhang[3], Peter Olson[3], Lin Chen[1], Terence K. Lee[4], Tan To Cheung[1], Chung Mau Lo[1], and Xiao Qi Wang[1,5]

Abstract

Aberrant activation of the Notch signaling pathway is implicated in many solid tumors, including hepatocellular carcinoma, indicating a potential use of Notch inhibitors for treatment. In this study, we investigated the antitumor and antimetastasis efficacy of the novel Notch inhibitor (γ-secretase inhibitor) PF-03084014 in hepatocellular carcinoma. Hepatocellular carcinoma spherical cells (stem-like cancer cells), a sphere-derived orthotopic tumor model and one patient-derived xenograft (PDX) model were used in our experiment. We demonstrated that PF-03084014 inhibited the self-renewal and proliferation of cancer stem cells. PF-03084014 reduced the hepatocellular carcinoma sphere-derived orthotopic tumor and blocked the hepatocellular carcinoma tumor liver to lung metastasis. We further tested the PF-03084014 in PDX models and confirmed the inhibition tumor growth effect. In addition, a low dose of PF-03084014 induced hepatocellular carcinoma sphere differentiation, resulting in chemosensitization. Antitumor activity was associated with PF-03084014-induced suppression of Notch1 activity, decreased Stat3 activation and phosphorylation of the Akt signaling pathway, and reduced epithelial–mesenchymal transition. These are the key contributors to the maintenance of cancer stemness and the promotion of cancer metastasis. Moreover, the Notch–Stat3 association was implicated in the clinical hepatocellular carcinoma prognosis. Collectively, PF-03084014 revealed antitumor and antimetastatic effects in hepatocellular carcinoma, providing evidence for the potential use of gamma-secretase inhibitors as a therapeutic option for the treatment of hepatocellular carcinoma. *Mol Cancer Ther; 16(8); 1531–43. ©2017 AACR.*

Introduction

The Notch pathway is evolutionarily conserved and plays fundamental roles in diverse developmental processes, from the self-reorganization of cell diversity to the differentiation and proliferation of stem/progenitor cells (1). Notch signaling regulates cell fate, behavior, proliferation, and morphology. Dysfunction of the Notch pathway contributes to multisystemic developmental defects. Alterations in the Notch pathway also contribute to a large number of hematopoietic and solid tumors. Aberrant regulation in cancers includes activating and inactivating mutations, receptor/ligand overexpression, epigenetic regulation, and effects of posttranslational modifications (1–3). On the basis of intense research of the Notch pathway in cancer, the Notch pathway has been developed as a potential molecular target for treatment of tumors. Various Notch targeting agents are in clinical trials including a Notch-specific antibody, DLL4-specific antibody, pan-Notch inhibitor, and gamma-secretase inhibitor (GSI) for the treatment of T-cell acute lymphoblastic leukemia (T-ALL), lymphoid malignancy, and advanced and metastatic solid tumors (2, 4). However, currently there is no FDA-approved Notch-targeting therapy (3). This is because (i) off-target Notch-associated effects of gastrointestinal toxicity; (ii) potential side effects affecting adult differentiation and regeneration of tissue; and (iii) distinct roles of Notch on tumorigenesis during different tumor stages, which might reduce the specificity and effects of Notch inhibitors (3).

Hypermalignant cancer cells, termed cancer stem cells (CSC) or stem-like cancer cells represent a distinct population that can be isolated from tumor tissues and exhibit long-term clonal repopulation and self-renewal capacity (5–7). They are highly active in generating new tumors upon implantation in animal models (8). Cancer cells are equipped with apoptotic blocks, high expression of drug transporters, efficient DNA repair, quiescence, and metastasis-forming potential, which are the mechanisms of therapy resistance. Interestingly, these mechanisms are also active in CSCs (9, 10). Drug resistance allows CSCs to survive conventional and even targeted therapies and is ultimately responsible for relapse (11). Thus, CSCs have become a therapeutic target of prime interest in drug discovery (12). A large number of signaling pathways have been demonstrated to be involved in the induction

[1]Department of Surgery, The University of Hong Kong, Hong Kong. [2]Department of Medicine, The University of Hong Kong, Hong Kong. [3]Oncology Research Unit, Pfizer Global Research and Development, La Jolla, California, USA. [4]Department of Applied Biology and Chemical Technology, The Hong Kong Polytechnic University, Hong Kong. [5]State Key Laboratory for Liver Research, The University of Hong Kong, Hong Kong.

Note: Supplementary data for this article are available at Molecular Cancer Therapeutics Online (http://mct.aacrjournals.org/).

Corresponding Author: Xiao Qi Wang, The University of Hong Kong, Sassoon No. 21, Li Ka Shing Faculty of Medicine, 999077, Hong Kong. Phone: 852-3917-9653; Fax: 852-3917-9634; E-mail: xqwang@hku.hk

doi: 10.1158/1535-7163.MCT-17-0001

and maintenance of CSCs, which are highly conserved pathways involved in development and tissue homeostasis, including Notch, Hedgehog (HH), and Wnt pathways (4). Therefore, these developmental pathways may be important therapeutic targets for the suppression of CSC self-renewal, proliferation, and tumor progression (4). Over the past few years, new investigational agents have been developed to target CSCs by inhibiting the Notch pathway, although robust antitumor activity has not yet been observed in clinical trials (4).

PF-03084014 (PF-4014) is a GSI developed by Pfizer, which shows antitumor efficacy in hematologic, breast, colorectal, and pancreatic cancer models (13–18), and suppresses hepatic metastases of neuroblastoma and breast cancer cells (19). Currently PF-03084014 is in phase I or phase II trials for the treatment of T-ALL, lymphoma, desmoid tumors, and fibromatosis (4, 20, 21). Although abnormal expression of the Notch pathway has been demonstrated in hepatocellular carcinoma (22), there is no reported study on the anticancer potential of Notch inhibitors on hepatocellular carcinoma from the cellular level to animal models *in vivo*. In this study, we demonstrated that PF-03084014 suppressed proliferation of hepatocellular carcinoma spherical cells (cancer stem-like cells) *in vitro*, hepatocellular carcinoma sphere-derived orthotopic tumor, and patient-derived xenograft (PDX) tumor growth *in vivo*. PF-03084014 also significantly blocked hepatocellular carcinoma tumor metastasis in hepatocellular carcinoma sphere-derived orthotopic tumor. Antitumor activity was associated with PF-03084014-induced suppression of the Notch1–Stat3 signaling, decreased phosphorylation of the Akt signaling pathway, and reversed epithelial–mesenchymal transition. Moreover, the Notch1–Stat3 association was significantly related with clinical hepatocellular carcinoma prognosis.

Materials and Methods

Cell culture, transfection, and hepatic cancer sphere assay

The hepatocellular carcinoma cell lines Huh7, PLC, Hep3B, and normal hepatocyte cell line MIHA from the ATCC were cultured in DMEM supplemented with 10% FBS (Life Technologies) at 37°C and 5% CO_2. The MHCC97H (97H) and MHCC97L (97L) cells from the Cell bank of Shanghai, Chinese Academy of Sciences, were isolated from a male metastatic hepatocellular carcinoma patient (23) and stably transfected with luciferase. The cell lines were obtained in the year of 2015. The vector-based siRNA-Notch1 stable transfection method was described in our previous paper (22). Liver cancer spheres were generated in DMEM:F12 (Life Technologies) supplemented with 2% B-27 (Life Technologies), EGF, bFGF (PeproTech), 100 IU/mL penicillin, and 100 μg/mL streptomycin on ultra-low attachment or polyHEMA-coated plates for 10 to 14 days. The Notch inhibitor PF-03084014 (Pfizer Global Research and Development; 0.5–1 μmol/L), Stat3 inhibitor JSI-124 (Merck; 1 μmol/L), and chemotherapy drug doxorubicin (dox; Main Luck Pharmaceuticals; 0.2 μg/mL), cisplatin (cis; MaynePharma, Melbourne; 0.5 μg/mL) were administered one to two times at the indicated doses.

Tumor model and drug administration

The 97L and 97H hepatocellular carcinoma monolayer cells (1×10^6) or 97H-derived spherical cancer cells (5×10^5) were subcutaneously injected into 4-week-old nude or SCID-beige mice. The 1 to 2 mm^3 subcutaneously formed tumor cubes were then implanted into the left liver lobes of nude mice as described previously (22). Fresh tumor was obtained from Queen Marry Hospital. The PDX models were built and the procedure have been described in previous article (24). The mice were randomized to the respective treatment groups. Either vehicle or PF-03084014 (dissolved in 0.5% methyl cellulose) was administered orally twice daily at 100 mg/kg for 6-day/per week in weeks 1, 2, 4, and 6. The size of the tumor and lung metastasis were monitored based on its luciferin (150 mg/kg, i.p. injection; Gold Biotechnology) signal in an IVIS Spectrum *in vivo* imaging system (PerkinElmer). At the end point (8 weeks), the size and weight of the tumor were measured. Tumor size was calculated using the formula: tumor volume $V = (L \times W \times W)/2$. All mouse experiments were approved by the Committee on the Use of Live Animals of the University of Hong Kong (CULATR 3091-13).

Western blot analysis and coimmunoprecipitation

Polyvinylidene difluoride membranes containing electrophoretically separated proteins from hepatocellular carcinoma tumor tissue and whole-cell lysates were probed with antibodies against cleaved Notch1, phospho-Stat3 (T705, S727), phospho-Akt (T308, S473), phospho-GSK3β (S9), phospho-Erk1/2 (T202/T204), Nanog, Oct4, Sox2 (all from Cell Signaling Technology), E-cadherin and Snail1 (Santa Cruz Biotechnology), and β-actin (Sigma-Aldrich). The resultant immune complexes were visualized using enhanced chemiluminescence detection reagents (Bio-Rad). The band density was analyzed by Image J software that has been described in our previous article (22). *In vitro* protein interaction was assessed on the basis of coimmunoprecipitation (co-IP) using cleaved Notch1 and total Stat3 antibodies. Briefly, 100 to 200 μg of total lysates from tumor tissue treated with vehicle or PF-03084014 was incubated with cleaved Notch1 antibody overnight. The immune complexes were analyzed by immunoblotting with anti-Stat3 antibody.

Flow cytometry

To identify the liver CSC population, the cells were labeled with antibodies against CD90-APC, EpCAM-PE-Cy7 (eBioscience), and the corresponding isotype antibody as a control to exclude nonspecific background staining. The stained cells were then subjected to flow cytometry analysis using FACSCalibur (Becton Dickinson).

qRT-PCR

Total RNA was extracted using an RNeasy Kit (Qiagen), treated with DNase I, and then reverse-transcribed with the Transcriptor First Strand cDNA Synthesis Kit (Roche). Quantitative PCR was performed using the Selected SYBR Green Master Mix (Life Technologies) on an ABI 7900HT Detection System. Primers used in this study were listed in Supplementary Table S1.

Clinical hepatocellular carcinoma specimens

Hepatocellular carcinoma tumor tissue specimens were collected from 39 hepatocellular carcinoma patients diagnosed with stage I to IV pathologic tumor–node–metastasis (TNM) disease. The samples were provided by the Tissue Bank at the Department of Surgery at Queen Mary Hospital. The collection and storage of clinical specimens for the Tissue Bank has been approved by the Institutional Review Board of the University of Hong Kong/Hospital Authority of Hong Kong (UW05-3597/I022).

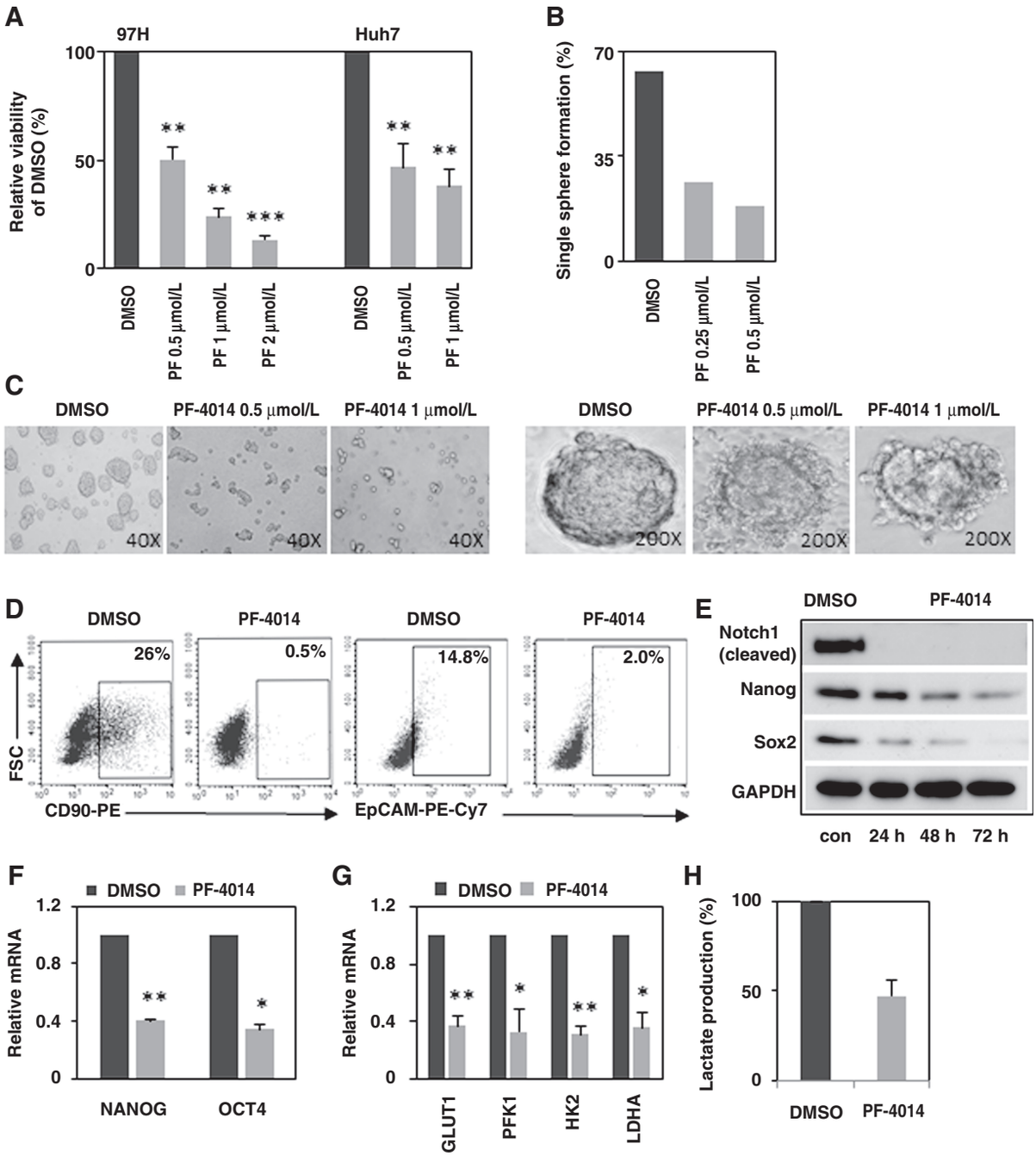

Figure 1.

PF-03084014 inhibits hepatocellular carcinoma sphere self-renewal and proliferation *in vitro*. **A,** Hepatocellular carcinoma 97H- and Huh7-derived sphere cells were treated with DMSO or PF-03084014 (0.5, 1, and 2 μmol/L). Sphere numbers were counted at 7 to 14 days. Relative viability was counted as PF-03084014 vs. DMSO groups. The data were presented as the mean ± SD, $n = 2$, from two independent experiments, each in triplicate. An independent t test was used for statistical comparison. *, $P < 0.05$; **, $P < 0.01$; ***, $P < 0.001$. **B,** The 97H spheres were serially diluted into single cells followed by PF-03084014 (0.25, 0.5 μmol/L) treatment. Single-cell formation was counted by single sphere seeding number versus sphere formation number. **C,** Phase contrast images of sphere colonies after DMSO or PF-03084014 treatment. **D,** Flow cytometry analysis of the $CD90^+$ and $EpCAM^+$ population in 97H spheres treated with DMSO or PF-03084014. **E,** Western blot analysis of protein levels of Nanog and Sox2 at 24, 48, and 72 hours in vehicle- and PF-03084014-treated 97H spheres. **F,** mRNA levels of the stemness genes NANOG and OCT4 in 97H spheres treated with PF-03084014 versus DMSO. qRT-PCR data are represented as the mean ± SD, $n = 2$, each in duplicate. **G,** qRT-PCR of glycolytic genes, *GLUT1, PFK1, HK2*, and *LDHA*. **H,** The 97H spheres were treated with PF-03084014 or DMSO, and the lactate concentration in the medium was quantified on day 3.

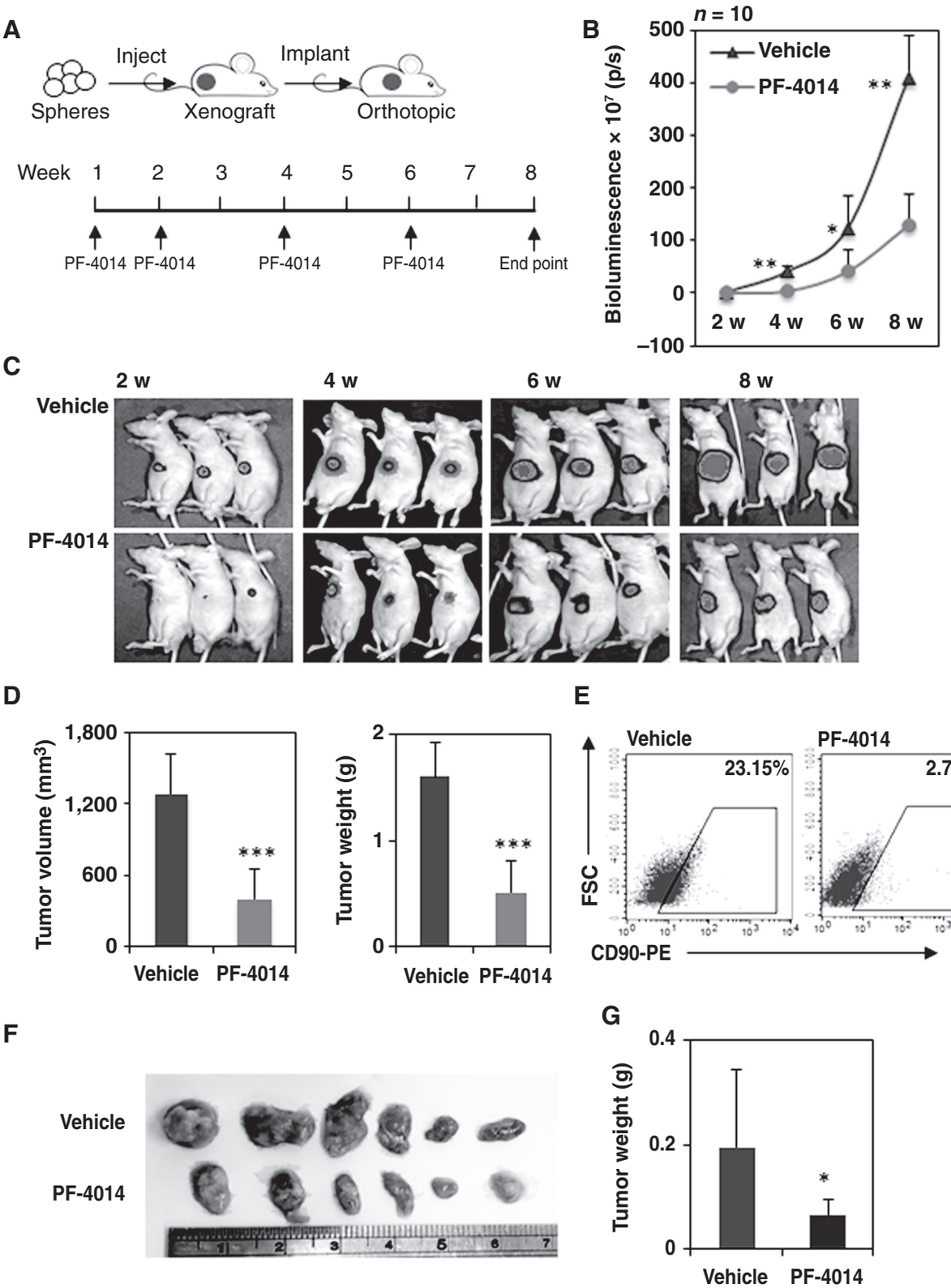

Statistical analysis

The results for variables are presented as the means ± SD. Treatment groups were compared with controls using a paired or independent Student *t* test. The association between cleaved Notch1 and pStat3 (T705) or pStat3 (S727) expression in hepatocellular carcinoma tumors was analyzed using a linear regression. Differences in hepatocellular carcinoma patient survival were assessed using a Kaplan–Meier analysis. The risk factors associated with the survival were assessed by univariate and multivariate analysis using the Cox proportional hazard regression model. All analyses were performed using SPSS 21 (IBM Corp.). A P value < 0.05 was considered statistically significant.

Results

PF-03084014 inhibits hepatocellular carcinoma spherical CSC self-renewal and proliferation

Notch signaling is one of the highly conserved pathways in developmental processes and stem cell fate regulation, which implies that it would be active in CSC regulation (4). A large number of Notch inhibitors have been developed for potential cancer treatments, although their roles in the suppression of CSCs have not been well defined. We investigated the anticancer efficacy of a GSI (PF-03084014) on a liver cancer anchorage-independent spherical cell model because CSCs can be enriched in spherical cells (25). We generated liver cancer spherical cells from 97H and Huh7 cells. The second and third generation of spheres from the dissected single spherical cells was used for all experiments. PF-03084014 suppressed sphere formation in a dose-dependent manner, leading to significantly reduced 97H-sphere viability (Fig. 1A). PF-03084014 moderately inhibited another hepatocellular carcinoma cells, including Huh7-derived sphere viability (Fig. 1A). Single sphere formation capacity of 97H spherical cell was reduced even with lower doses of PF-03084014 (Fig. 1B), indicating significant suppression of sphere proliferation (Fig. 1A–C). PF-03084014 decreased the populations of $CD90^+$ and $EpCAM^+$ cells, which are liver CSC markers (Fig. 1D) (26). Similarly, expression of stemness-associated genes and proteins NANOG, OCT4, and SOX2 were also decreased (Fig. 1E and F). A high rate of glycolysis is a metabolic signature of CSCs (Warburg effect version 2.0) (27). PF-03084014 significantly reduced glycolytic gene expression (Fig. 1G) and the glycolytic rate consequently, as measured by lactate production in CSC sphere medium (Fig. 1H). These results suggest that inhibition of hepatocellular carcinoma spherogenesis by PF-03084014 resulted from inhibition of CSC self-renewal capacity. Interestingly, inhibition effects of PF-03084014 were shown in hepatocellular carcinoma cells with high Notch1 expression (97L and 97H) (22) but not on low or no Notch expression Hep3B and PLC cells. Moreover, PF-03084014 did not suppress normal hepatocyte MIHA proliferation (Supplementary Fig. S1A–S1C).

PF-03084014 inhibits hepatocellular carcinoma-sphere derived orthotopic tumor and PDX tumor growth

To investigate whether the *in vitro* impact of PF-03084014 on hepatocellular carcinoma spherical CSCs can be extended to *in vivo* models, an orthotopic hepatocellular carcinoma model was generated from 97H spherical CSCs (Fig. 2A) to determine the efficacy of PF-03084014 *in vivo*. Orthotopic tumor models are considered more clinically relevant and a better predictive model of drug efficacy. Hepatocellular carcinoma is known as an aggressive and highly resistant cancer, we therefore modified administration by 100 mg/kg of PF-03084014 for 6 days/week, and total administration occurred over 4 weeks (Fig. 2A). Under this relatively higher dose of PF-03084014 administration, the mouse body weight of the treatment group decreased by 23%–20% at week 2 and 3, 12%–10% at week 4 and 5, 6%–4% at week 6 and 7, and 0% at week 8 compared with the vehicle group, indicating a trend of GSI tolerance (Supplementary Fig. S2).

Using bioluminescence to trace the tumor growth, we found that tumor growth was reduced by 75%, 87%, 67%, and 68.5% at week 2, 4, 6, and 8, respectively, in the PF-03084014 group compared with the vehicle group (Fig. 2B and C). Similarly, PF-03084014 decreased tumor volume at the endpoint by 69% (Fig. 2D, left) and decreased tumor weight by 68% (Fig. 2D, right). Consistent with the *in vitro* result that PF-03084014 targets the hepatocellular carcinoma CSC population (Fig. 1D), the liver cancer CSC $CD90^+$ population in the remaining tumor tissue was 2.76%, which was a 8.4-fold dramatic decrease compared with control with 23.15% high CSCs population (Fig. 2E). The results indicate that PF-03084014 is able to inhibit the CSC population in the tumor mass to suppress tumor growth. Application of PDX model is a novel method to predict antitumor efficacy, next we confirmed the inhibition effect of PF-03084014 on tumor growth which is consistent with spherical cell–derived orthotopic tumor models (Fig. 2F and G). In the 97H hepatocellular carcinoma monolayer cell–generated orthotopic model and 97L hepatocellular carcinoma monolayer cell–derived xenograft model, PF-03084014 also displayed antitumor effects with tumor volumes decreasing by 60% in the orthotopic model (Supplementary Fig. S3A–S3D), and by 48.3% in the xenograft model (Supplementary Fig. S3E). The data also indicated that administration of PF-03084014 for 4 weeks (Supplementary Fig. S3D) was more effective in inhibition of tumor growth than administration of PF-03084014 for 2 weeks (Supplementary Fig. S3E).

Notable effects of PF-03084014 in blocking hepatocellular carcinoma metastasis *in vivo*

Tumor metastasis is a major contributor to the death of cancer patients. Intrahepatic and extrahepatic metastasis occurs in more than half of hepatocellular carcinoma patients even after surgical resection, leading to poor prognosis (28, 29). Our previous study demonstrated that knockdown of Notch1 reduced hepatocellular carcinoma metastasis *in vivo* (22). Here we administered

Figure 2.

Anticancer effects of PF-03084014 in the hepatocellular carcinoma sphere-derived orthotopic models. **A,** Schematic of the experimental setup. The 97H sphere-generated subcutaneous tumor cubes were implanted in the left liver lobes of nude mice. One week after tumor implantation, the mice with a positive luciferin signal were randomized and treated with vehicle and PF-03084014, as shown in the schematic setup of the drug administration. **B,** Tumor growth kinetics and statistical comparison based on the luciferin bioluminescence signal at 2, 4, 6, and 8 weeks. Data are the mean ± SD, $n = 10$. *, $P < 0.05$; **, $P < 0.01$. **C,** Representative tumor images based on the luciferin bioluminescence of B. **D,** Statistical comparison of the tumor volume (left) and tumor weight (right) at the endpoint (8 weeks). ***, $P < 0.001$. **E,** The tumor tissue was digested at the end of study to detect the $CD90^+$ population by flow cytometry. **F,** PDX tumor Image of hepatocellular carcinoma mice were subjected to 4 weeks of vehicle or PF-03084014 (100 mg/kg for 6-day/per week) treatment. **G,** PDX tumor weights were statistically compared at the endpoint (4 weeks).

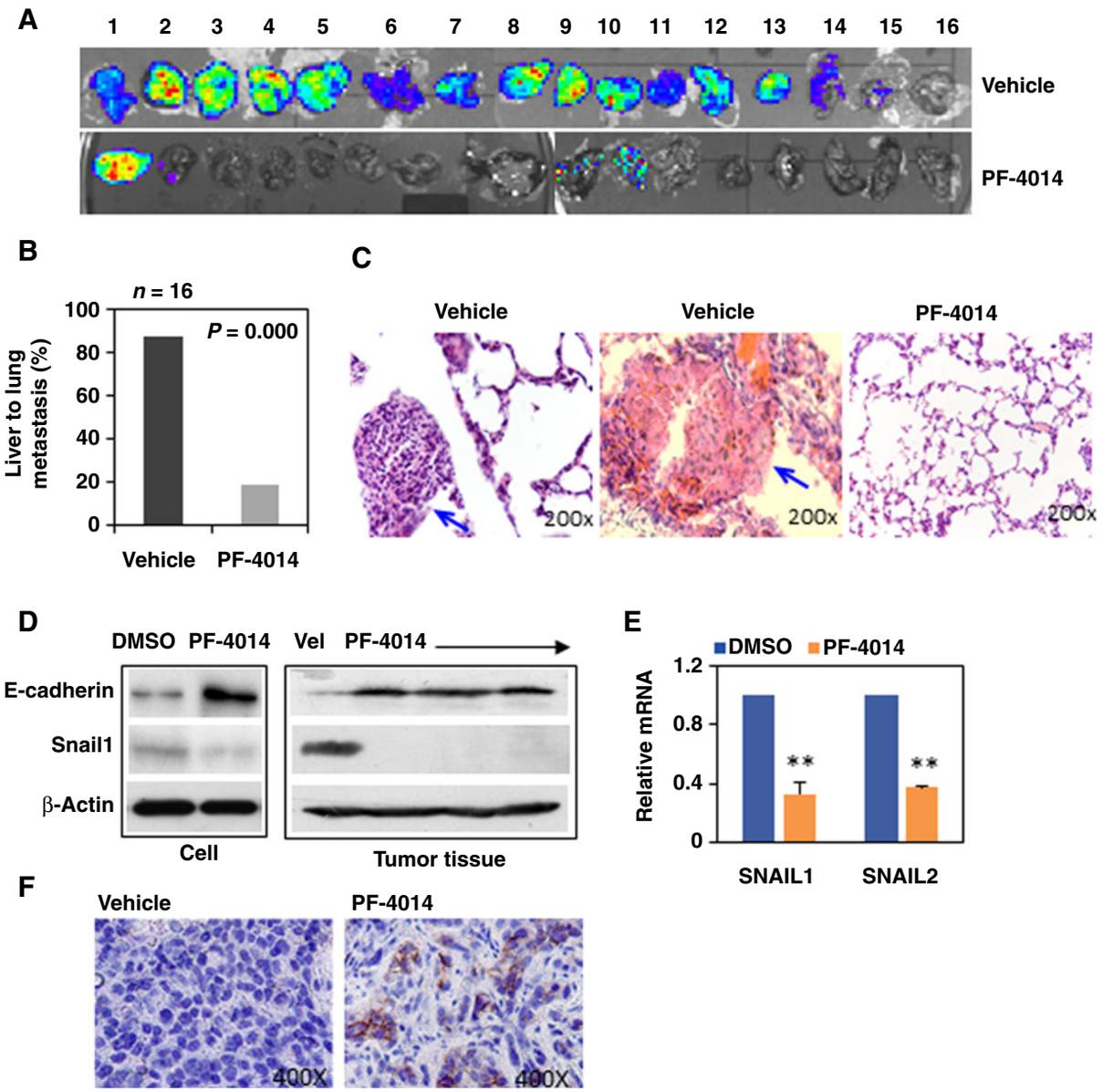

Figure 3.

PF-03084014 blocks hepatocellular carcinoma orthotopic tumor metastasis from the liver to the lung. **A,** Subcutaneously formed tumors from 97H spheres ($n = 8$) or 97H monolayer cells ($n = 8$) were implanted into the left liver lobes in nude mice followed by vehicle or PF-03084014 treatment. At the end of the study, mouse lung was isolated after intraperitoneal injection of luciferin (25 mg/kg) and the liver tumor luciferin signal was detected under an IVIS Spectrum. Liver tumor luciferase signals in a total of 16 mice from the vehicle (up panel) and PF-03084014 (lower panel) groups are shown. **B,** Based on A, the percentage of liver to lung metastasis was calculated. **C,** H&E staining of representative lung tissue sections. Arrows indicate liver tumor lesions and surrounded infiltrating cells. **D,** Western blots of the EMT markers E-cadherin and Snail1 in 97H spheres and in tumor tissue treated with vehicle and PF-03084014. **E,** mRNA levels of SNAIL1 and SNAIL2 in 97H spheres treated with vehicle and PF-03084014. **F,** IHC detected E-cadherin in vehicle- and PF-03084014-treated 97H sphere-derived tumor tissues.

PF-03084014 in the same hepatocellular carcinoma orthotopic tumor model derived from 97H sphere and monolayer cells, where 97H cells are isolated from the primary hepatocellular carcinoma metastatic tumor tissue with a high metastatic rate from the liver to the lung in the mouse (23). At the 8-week endpoint, the mouse lung was dissected to detect the luciferin signal under an IVIS Spectrum. PF-03084014 treatment dramatically decreased hepatocellular carcinoma liver to lung metastasis with only 3 of 16 (18.8%) animals showing lung metastasis, whereas metastasis rate remained high (87.5%) in the vehicle treatment group (Fig. 3A and B). Hepatocellular carcinoma tumor tissue in the lung was further confirmed by the lung section observation (Fig. 3C). These results not only further supported our previous results that abnormal Notch1 is a contributor to liver cancer metastasis (22), but they also demonstrated a possibility that a Notch inhibitor can be used for the treatment of metastatic

cancer. To further understand the mechanisms, we found that a high level of mesenchymal markers, such as Snail1 and Snail2, were significantly reduced in 97H cells and abolished in the 97H tumor by PF-03084014, whereas the epithelial marker E-cadherin was enhanced (Fig. 3D–F). Thus, suppressed metastasis by PF-03084014 might occur through inhibition of Notch1 to reverse EMT phenotypes.

Low doses of PF-03084014 induce hepatocellular carcinoma sphere differentiation and chemosensitization

PF-03084014 induced dose-dependent inhibition of hepatocellular carcinoma sphere proliferation, where the inhibition by low doses of PF-03084014 was moderate with 50% of the spheres surviving (Fig. 1A). However, more than 40% of these surviving spheres were in differentiated states (Fig. 4A), leading to an

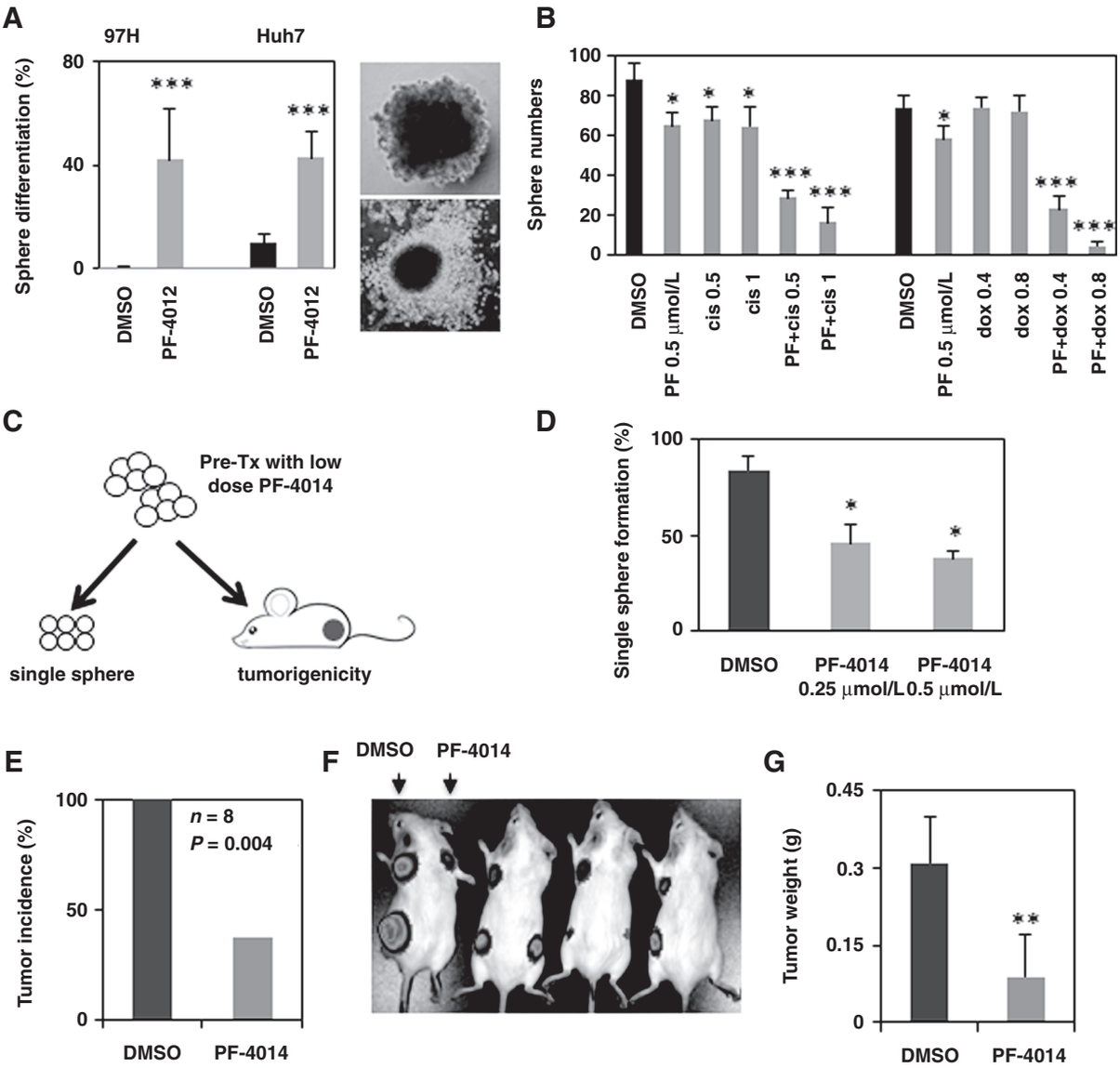

Figure 4.

PF-03084014 induces hepatocellular carcinoma sphere differentiation. **A,** Differentiation is the formation of other noncancer stem cells from the undifferentiated precursor cancer stem cells. 97H spheres and Huh7 spheres were treated with DMSO or a low dose of PF-03084014 (0.25–0.5 μmol/L). The percentage of differentiated spheres were counted and statistically compared. **B,** The sphere number of 97H spherical cells treated with PF-03084014 (0.5 μmol/L), cis (0.5 μg/mL or 1 μg/mL), or dox (0.4 μg/mL or 0.8 μg/mL) alone and cells treated with PF-03084014 (0.5 μmol/L) in combination with cis (0.5 μg/mL or 1 μg/mL) or dox (0.4 μg/mL or 0.8 μg/mL) are shown. **C,** Pretreatment with PF-03084014 *in vitro* decreased the tumorigenicity of hepatocellular carcinoma spheres *in vivo*. Schematic of the experimental setup of pretreatment. The 97H spheres were pretreated with PF-03084014 (0.25–0.5 μmol/L) or DMSO, followed by single sphere formation and *in vivo* tumorigenicity assays without further treatment. **D,** Statistical comparison of single sphere formation after pretreatment. **E,** Xenograft tumor incidence (%) at 6 weeks after the injection of pretreated cells ($n = 8$). **F,** Representative tumor size based on bioluminescence imaging. DMSO or PF-03084014–pretreated cells were injected into the same mouse for comparison. **G,** Statistical comparison of tumor volume at the endpoint. *, $P < 0.05$; **, $P < 0.01$; ***, $P < 0.001$.

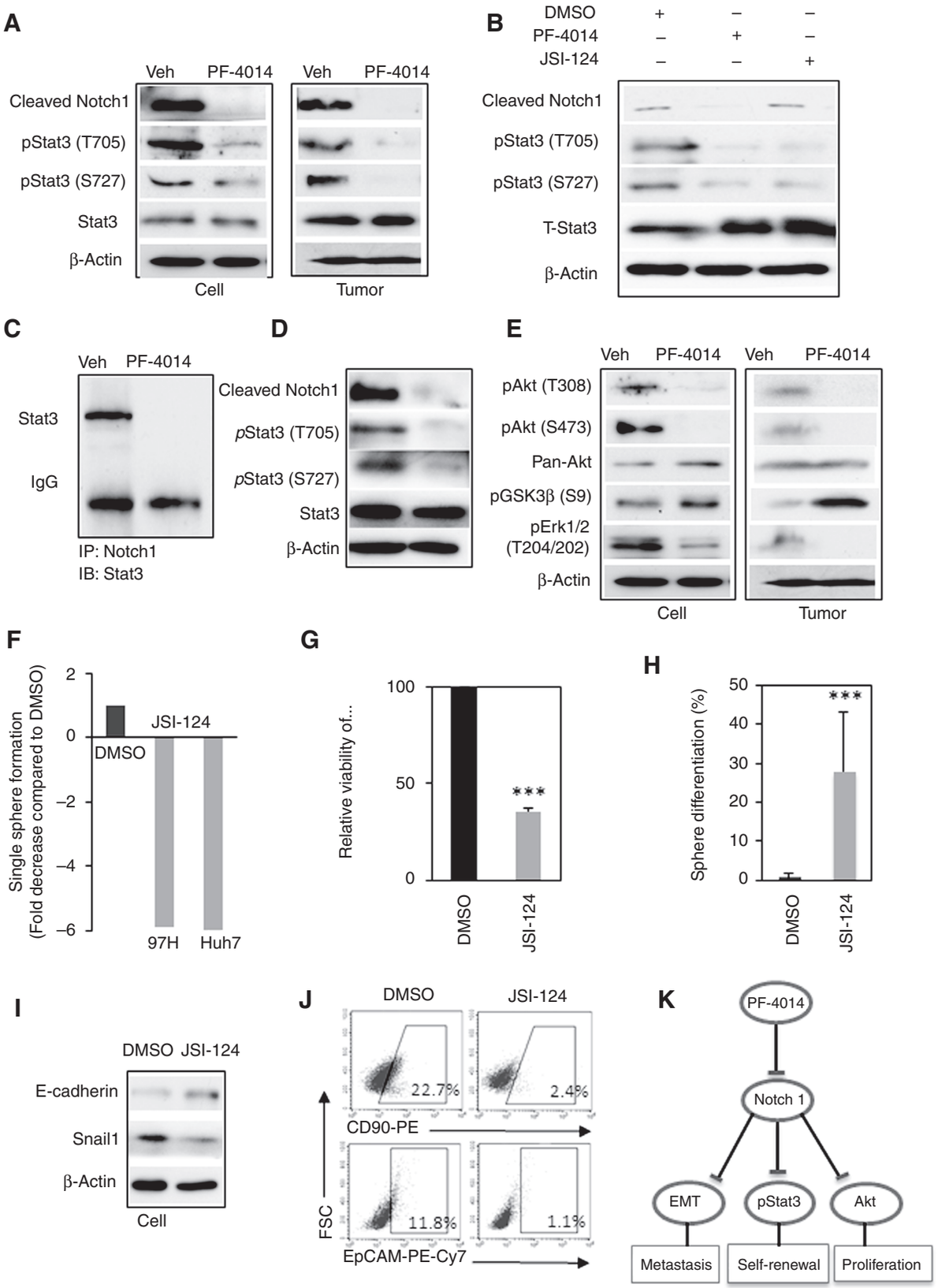

expectation that these cells may become sensitized to chemotherapy. We then determined the effect of PF-03084014 on the responsiveness to the conventional therapy drugs cisplatin and doxorubicin. For 97H spheres, the survival rate with cisplatin and doxorubicin were similar to DMSO-treated control cells; however, in combination with 0.5 μmol/L PF-03084014, responsiveness to chemotherapy drugs was significantly enhanced by 39% or 51% at levels of cisplatin 0.5 μg/mL or doxorubicin 0.4 μg/mL, respectively, and by 48% or 68% at levels of cisplatin 1 μg/mL or doxorubicin 0.8 μg/mL, respectively (Fig. 4B). These data suggest that low doses of PF-03084014 are able to induce CSC differentiation, which could be a critical state in turning highly resistant CSCs into therapy-sensitive cells.

Notch inhibition reduces CSC self-renewal *in vitro* and tumorigenicity *in vivo*

Next, we assessed the *in vivo* tumorigenicity of cells pretreated with Notch inhibitor. Prior to injection, 97H spheres were exposed to DMSO or a low dose of PF-03084014 *in vitro*. All surviving cells were subjected to single cell sphere formation or SCID mice for xenograft tumor formation (Fig. 4C). No further *in vivo* treatment was administered. The single-cell sphere formation rate was 84% in the DMSO-pretreated group versus 46% and 38% in the 0.25 or 0.5 μmol/L PF-03084014-pretreated groups, respectively (Fig. 4D). In addition, the self-renewal ability of 97H spheres, were continuously verified and confirmed by the spherical formation and the expression of stemness markers (CD90 and EpCAM) after repeated dispersion and passage. Xenograft tumorigenicity was determined at 6 weeks. *In vitro* PF-03084014 pretreatment significantly decreased tumorigenicity *in vivo* by reducing the tumor incidence, which was 100% in the DMSO group and 37.5% in the PF-03084014 group; Notch inhibitor pretreatment also significantly reduced tumor weight (Fig. 4E–G; Supplementary Fig. S4). Therefore, PF-03084014 can drive hepatocellular carcinoma CSCs into a more differentiated state that is sensitive to chemotherapy at the cellular level and, more importantly, minimizes tumorigenicity at the *in vivo* xenograft tumor level.

PF-03084014 impairs the Notch pathway and modulates Stat3

As PF-03084014 targets γ-secretase, we examined Notch activation, including the expression of cleaved Notch 1 intracellular domain (NICD), Notch ligand Delta-like-ligand 1 (DLL1), and Notch target gene HEY1 in sphere cells and sphere-derived tumor tissues. PF-03084014 suppressed activated Notch1 expression (Fig. 5A). PF-03084014 also decreased mRNA expression of Notch1, DLL1, and HEY1 (Supplementary Fig. S5).

The Notch pathway cross regulates with many other signaling pathways. Accordingly, we detected the related proteins in the pathways that interact with Notch signaling. PF-03084014 treatment significantly decreased phosphorylation of Stat3 at Tyr 705 and Ser 727 in both 97H spheres (Fig. 5A, left) and 97H sphere-derived tumor tissue (Fig. 5A, right) compared with DMSO or vehicle treatment groups. To confirm the inhibition of PF-03084014 on Stat3, we compared the phosphorylation states of Stat3 under treatment with the Stat3 inhibitor (JSI-124) (30) and PF-03084014. PF-03084014 treatment alone inhibited activation of Notch1, where phosphorylation of Stat3 at T705 and S727 was also reduced, which is similar to the decreased pStat3 induced by JSI-124 (Fig. 5B). The result indicates a Notch1–Stat3 axis, where decreased pStat3 by PF-03084014 occurs via the reduction in Notch1. Given that cleaved Notch1 is localized to the nucleus and Stat3 maintains a prominent nuclear presence (31), we performed a coimmunoprecipitation. As shown in Fig. 5C, Notch1 clearly interacts with Stat3. Next we further verified Notch1–Stat3 association by transfection knockdown Notch1, which revealed that down-regulation activated Notch1 was associated with reduced pStat3 at T705 and S727 (Fig. 5D). When Notch1 protein expression was inhibited by PF-03084014, it brought down with almost no pStat3. The result is further verification that GSI can inhibit the activation of Stat3. PF-03084014 also impaired Erk phosphorylation (Fig. 5E). Moreover, phosphorylation of the PI3K/Akt signaling pathway was inhibited, as shown by a decrease in pAkt (T308), pAkt (S473), and an increase in pGSK3β at Ser9 (an inactivated form of GSK3β; Fig. 5E), which in some degrees is consistent with our previous finding in human embryonic stem cells demonstrated that these signaling are essential in stem cell self-renewal capacity, proliferation, and differentiation (32). Hence, PF-03084014 may also inhibit cancer stem cell self-renewal capacity, proliferation as well as inducing differentiation through these signaling.

Stat3 is a transcriptional factor that is constitutively active in many human cancers (33–35). Recently, it was demonstrated that Stat3 is an important factor for maintaining cancer stemness (7). We next determined the effect of the Stat3 inhibitor on hepatocellular carcinoma spherical CSCs. Application of the Stat3 inhibitor JSI-124 significantly suppressed the overall and, more importantly, single spherical colony formation in two cell lines (Fig. 5F and G). Surviving spheres were mostly in differentiated states (Fig. 5H). Moreover, JSI-124 treatment decreased the proportion of $CD90^+$ and $EpCAM^+$ cells compared with DMSO-treated cells (Fig. 5J). JSI-124 also reversed EMT by enhancing E-cadherin and decreasing Snail1 expression (Fig. 5I). The data suggest that inhibition of Stat3 impairs self-renewal and proliferation of

Figure 5.

PF-03084014 modulates Stat3 to suppress hepatocellular carcinoma CSCs. **A,** Western blot analysis of protein levels of cleaved Notch1, pStat3 (T705), and pStat3 (S727) in vehicle- and PF-03084014-treated 97H spheres and endpoint 97H sphere-derived tumor tissues. **B,** The 97H spheres were treated with DMSO, PF-03084014, or JSI-124 (Stat3 inhibitor), followed by measurement of the protein levels of cleaved Notch1 and pStat3. **C,** Endpoint tumor tissue lysates were immunoprecipitated with cleaved Notch1 antibody; the bound proteins were analyzed using a Stat3 antibody. IgG was used as an internal loading control. **D,** Vector-based siNotch1 and siControl were stably transfected into hepatocellular carcinoma cells and the protein levels of cleaved Notch1, pStat3(T705), and pStat3 (S727) were analyzed by Western blot analysis. **E,** Western blot analysis of protein levels of pAkt at T308 and S473, pGSK3β, and pErk1/2 in vehicle- and PF-03084014-treated 97H spheres and endpoint tumor tissues. **F,** Single sphere formation capacity in 97H and Huh7 spheres treated with JSI-124 vs. DMSO. The single sphere formation in DMSO was defined as the fold decrease in the JSI-124 group was calculated as the inverse of the fold change. **G,** Relative sphere viability of 97H spheres treated with the Stat3 inhibitor JSI-124 (1 μmol/L) vs. DMSO. **H,** Percentage of differentiated spherical colonies after JSI-124 treatment. ***, $P < 0.001$. **I,** Western blot analysis of protein levels of E-cadherin and Snail1 in vehicle- and PF-03084014-treated 97H spheres. **J,** Flow cytometry analysis of the $CD90^+$ and $EpCAM^+$ population in 97H spheres after treatment with DMSO or JSI-124. **K,** Model of inhibition of Notch1 by PF-03084014 impairs CSC self-renewal, proliferation, and metastasis via suppression of Stat3, Akt signaling, and reversion of EMT, respectively.

hepatocellular carcinoma cancer spherical cells. The Notch pathway cross regulates multiple signaling pathways, where GSI inhibition of CSC self-renewal might occur via targeting of Stat3, one of the critical molecules in maintaining CSC stemness (7). Together, Notch inhibition by PF-03084014 impairs self-renewal and proliferation of hepatocellular carcinoma spherical CSCs, resulting in suppression of tumor growth and metastasis, which possibly occurs through suppression of Stat3, Akt, and reversal of EMT (Fig. 5K).

Association between Notch1 and Stat3 in hepatocellular carcinoma patients

Based on the possibility that suppression of hepatocellular carcinoma spherical cancer cells or cancer sphere-derived tumor growth by PF-03084014 might be through direct or indirect inhibition of Stat3, and the knowledge that Stat3 is consistently expressed in many types of cancers, we next assessed the association of Notch1 and Stat3 in hepatocellular carcinoma primary tumor tissues. We measured the protein levels of cleaved Notch1 and the phosphorylation of Stat3 (T705, S727) in 39 hepatocellular carcinoma tumor tissues. As shown in Fig. 6A, many hepatocellular carcinoma patients expressed high levels of the three tested proteins; 62% of hepatocellular carcinoma patients displayed significant Notch1-dependent pStat3 (T705) expression ($P = 0.000$; Fig. 6B, left), and 59% of patients exhibited Notch1-dependent pStat3 (S727) expression ($P = 0.000$; Fig. 6B, right), which support the interaction between Notch1 and Stat3 (Fig. 5C). Clinically, activated Notch1 levels were significantly associated with late-stage hepatocellular carcinoma, tumor size, venous infiltration, and 1- or 5-year recurrence, which is consistent with our previous study detected by mRNA expression of Notch1 in hepatocellular carcinoma (22). More importantly, hepatocellular carcinoma patients with aberrantly high Notch1 expression had a predicted disease progression and worse overall and disease-free survival ($P = 0.027$–0.000; Fig. 6C). Univariate analysis showed that in late stages of hepatocellular carcinoma, venous infiltration and high expression of activated Notch1 are the factors relating to patient survival. Among these significant factors, only aberrant expression of Notch1 is a significant independent factor relating to disease-free survival according to the multivariate analysis (Supplementary Table S2).

The next question we asked is whether the correlation between Notch1 and Stat3 can predict hepatocellular carcinoma progression. We defined Notch1/pStat3-related hepatocellular carcinoma cases as cases where the ratio of the two proteins (Notch1 vs. pStat3) was 0.5 to 1 and hepatocellular carcinoma cases of unrelated Notch1/pStat3 as cases where the ratio was less than 0.5 or larger than 1. Kaplan–Meier analysis illustrated that patients with Notch1/pSTAT3 (T705) related expression was remarkably associated with poor disease-free survival (log-rank $= 7.236$, $P = 0.007$; Fig. 6D), but was not significantly associated with poor overall survival (log-rank $= 3.197$, $P = 0.074$). Patients with Notch1/pSTAT3 (S727) related expression had a strong association with poor overall survival (log-rank $= 9.885$, $P = 0.002$) and poor disease-free survival (log-rank $= 13.425$, $P = 0.000$; Fig. 6E). These clinical results indicated an aberrant Notch1-dependent activation of Stat3 in hepatocellular carcinoma patients, which not only predicted a poor prognosis but also provided an option for using a Notch inhibitor such as PF-03084014 for treatment.

Discussion

In this study, we demonstrated that using a GSI to target Notch signaling has both antitumor and antimetastasis effects on hepatocellular carcinoma. In hepatocellular carcinoma spherical cancer cells *in vitro* and cancer stem-like cell-derived orthotopic tumor and PDX tumor models *in vivo*, we further demonstrated that GSI-mediated antitumor activity was associated with the inhibition of cancer CSC self-renewal and proliferation and the reversal of EMT phenotypes. PF-03084014 also induced spherical CSC differentiation leading to chemosensitization and reduced tumorigenicity. Moreover, the GSI suppressed multiple CSC promoting pathways. In particular, PF-03084014 inhibited the phosphorylation of Stat3, and the Notch1–Stat3 association was significantly related to hepatocellular carcinoma disease progression. These results provide (i) the first evidence of inhibition of Notch signaling by PF-03084014, which may have therapeutic potential for the treatment of hepatocellular carcinoma as well as metastatic hepatocellular carcinoma, and (ii) evidence that the GSI PF-03084014 is capable of targeting CSC self-renewal and proliferation directly or indirectly by targeting CSC-promoting genes.

There is increasing evidence that aberrant Notch pathway activation occurs in solid tumors, including liver cancers (36). In clinical hepatocellular carcinoma tumor tissues, upregulation of Notch components has been observed, which is significantly associated with disease progression such as tumor metastasis (22). Consistently, our current results demonstrated for the first time that using a GSI for pharmacologic inhibition of the Notch signaling pathway could have antitumor and antimetastasis effects in hepatocellular carcinoma *in vivo* models. GSIs are known to be toxic, as they are not cell-selective or system-specific (37). We observed that liver cancer cells with higher Notch expression (22) are more sensitive to GSI inhibition than liver cancer cells with lower Notch expression. Importantly, proliferation of the normal hepatocyte cell line MIHA was completely unaffected. Moreover, based on mice body weights, the PF-03084014 toxicity was generally limited and tolerable given that in our experimental setting, the total GSI administration was intermittent but relatively high in dose. Taken together, PF-03084014 seems to selectively target high Notch1-expressing cancer cells and is not associated with any signs of adverse effects on normal hepatocytes.

Constitutive activity of Notch1 in mouse embryonic hepatoblasts results in hepatocellular carcinoma development with 100% penetrance and a Notch gene signature of these tumors is also found in human hepatocellular carcinoma (38). These studies also suggest that persistent activation of the Notch signaling might play roles both in reprograming hepatic progenitor cells (HPC) into CSCs and in maintaining CSC features during hepatocellular carcinoma development (36). In our study design, the experiment was performed on liver cancer spheres, which enrich the hepatocellular carcinoma CSC population (25), and the *in vivo* orthotopic tumor model was also generated from hepatocellular carcinoma cancer spheres. Thus, it is basically an examination of GSI-mediated inhibition of CSC proliferation in a liver cancer model. The observation that PF-03084014 is able to inhibit hepatocellular carcinoma CSC sphere proliferation and orthotopic tumor growth is likely a result of PF-03084014 being able to impair CSC self-renewal. In addition, it seems that tumor growth

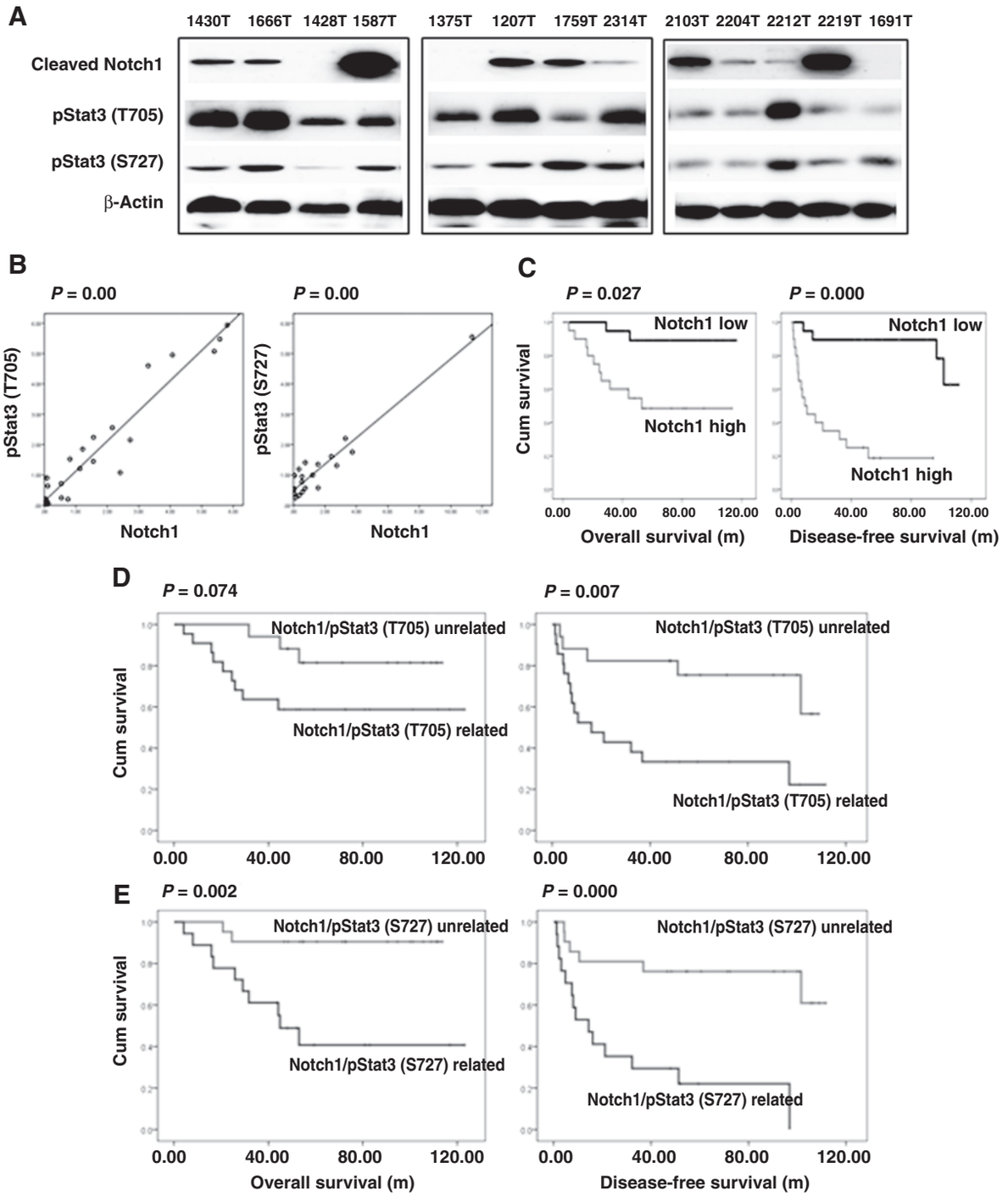

Figure 6.

Clinical association of Notch1 and pStat3 in hepatocellular carcinoma. **A,** Representative Western blots of cleaved Notch1, pStat3 (T705), pStat3 (S727), and β-actin from 39 hepatocellular carcinoma primary tumor tissues. **B,** Linear regression analysis of the Notch1-dependent expression of pStat3 (T705; left) and pStat3 (S727; right) using quantification of data from **A**. **C,** Kaplan–Meier analysis of the overall survival (left panel) and disease-free survival (right panel) of hepatocellular carcinoma patients in comparison with high and low Notch1 expression. **D,** Based on quantification of protein levels, hepatocellular carcinoma cases were defined as Notch1/pStat3-related when the ratio (Notch1 vs. pStat3) was 0.5 to 1, whereas hepatocellular carcinoma cases were considered Notch1/pStat3-unrelated when the ratio was <0.5 or >1. Kaplan–Meier analysis of the overall (left panel) and disease-free (right panel) survival of hepatocellular carcinoma patients with related versus unrelated Notch1/pStat3 (T705). **E,** Kaplan–Meier analysis of the overall and disease-free survival of hepatocellular carcinoma patients with related versus unrelated Notch1/pStat3 (S727).

reduction by PF-03084014 is more significant in hepatocellular carcinoma sphere-generated tumors than in hepatocellular carcinoma monolayer-generated tumors. Thus, impairing the self-renewal and stemness of CSCs is more effective for inhibition of tumor growth, as cancer stemness is the root of the tumor-forming capacity.

The treatment of hepatocellular carcinoma by conventional chemotherapy remains a therapeutic challenge, as hepatocellular carcinoma is a highly chemoresistant cancer and a subgroup of hepatocellular carcinoma is even resistant to molecular targeting agents such as sorafenib (39). Our observation that a low dose of PF-03084014 in combination with treatment with cis or dox can reach an inhibition rate of 80% to 90% in liver cancer spheres, indicating that targeting Notch can enhance chemosensitization of hepatocellular carcinoma. One potential mechanism could be that targeting Notch induces liver CSC differentiation, a critical cellular state for chemosensitization. More importantly, CSC differentiation by PF-03084014 deteriorates tumorigenicity by 62.5%. Thus, PF-03084014 inhibits Notch activity leading to chemosensitization through suppression of CSC stemness and induction of CSC differentiation.

Tumor metastasis is a major contributor to hepatocellular carcinoma cancer relapse and patient death. The previous evidence from primary hepatocellular carcinoma patients and *in vivo* hepatocellular carcinoma metastasis models (22) that Notch signaling is involved in hepatocellular carcinoma metastasis are further supported by the observation that PF-03084014 could effectively block lung metastasis in an hepatocellular carcinoma orthotopic model. One obvious mechanism which PF-03084014 suppressed *in vivo* metastasis was through reduction of Notch-mediated EMT by decreasing the level of the mesenchymal-associated molecules Snail1 and Snail2 and increasing the level of epithelia-associated molecules E-cadherin. The notable ability of PF-03084014 to block *in vivo* hepatocellular carcinoma metastasis provides strong evidence for the potential use of GSIs for the treatment of advanced hepatocellular carcinoma.

Under PF-03084014 treatment, phosphorylation of Stat3 at S705 and T727 were clearly inhibited and the interaction between Notch1 and Stat3 was abolished. Therefore, among multiple pathways regulated by Notch signaling, we demonstrated the Notch1–Stat3 association in hepatocellular carcinoma cells and primary tumors. It has been shown that Notch signaling induces activation of Stat3 and Akt to promote normal stem cell expansion (40), whereas Stat3 is a key driver of cancer stemness (31). Thus, Notch regulation of CSCs might be through Stat3 and the Notch1–Stat3 axis and may contribute to liver CSC self-renewal and proliferation that further drives tumor growth. Importantly, the Notch1–Stat3 association was demonstrated in hepatocellular carcinoma primary tumors and was a significant indicator of poor prognosis, suggesting that the Notch1–Stat3 axis might play a role in maintaining the CSC population in the tumor mass to support hepatocellular carcinoma growth. The evidence that PF-03084014 inhibited both Notch1 and Stat3 and blocked hepatocellular carcinoma metastasis *in vivo* indicates that GSIs have potential for the treatment of advanced hepatocellular carcinoma.

In summary, this research identified that the inhibition of Notch signaling using PF-03084014 had an antitumor and anti-metastatic effect in the hepatocellular carcinoma sphere-derived orthotopic model. The antitumor effect of PF-03084014 was confirmed by our PDX models. Furthermore, PF-03084014 inhibited hepatocellular carcinoma CSC self-renewal and proliferation via inhibition of the Notch1–Stat3 axis, where the Notch1–Stat3 association was significantly implicated in a poor hepatocellular carcinoma prognosis. PF-03084014 also induced CSC differentiation leading to chemosensitization. These findings suggest that PF-03084014 might have the potential for the treatment of advanced hepatocellular carcinoma.

Disclosure of Potential Conflicts of Interest

P. Olson is a Principle Scientist at Pfizer. No potential conflicts of interest were disclosed by the other authors.

Authors' Contributions

Conception and design: C.X. Wu, C.C. Zhang, X.Q. Wang
Development of methodology: C.X. Wu, C.C. Zhang, L. Chen
Acquisition of data (provided animals, acquired and managed patients, provided facilities, etc.): C.X. Wu
Analysis and interpretation of data (e.g., statistical analysis, biostatistics, computational analysis): C.X. Wu, X.Q. Wang
Writing, review, and/or revision of the manuscript: C.X. Wu, A. Xu, X.Q. Wang
Administrative, technical, or material support (i.e., reporting or organizing data, constructing databases): P. Olson, L. Chen, T.T. Cheung, C.M. Lo
Study supervision: A. Xu, T.T. Cheung, C.M. Lo, X.Q. Wang
Other (providing reagents for the experiments): T.K. Lee

Acknowledgments

We thank Dr. Yu (HBP, Queen Mary Hospital) for providing clinical tumor tissue support. We thank Jeason and Sally Li for outstanding technical support and Jana Wo for animal relevant information and technical support.

Grant Support

This study was supported by Healthy and Medical Research Fund, Research Council of Hong Kong (03143396 to X.Q. Wang).

The costs of publication of this article were defrayed in part by the payment of page charges. This article must therefore be hereby marked *advertisement* in accordance with 18 U.S.C. Section 1734 solely to indicate this fact.

Received January 3, 2017; revised March 29, 2017; accepted May 1, 2017; published OnlineFirst May 1, 2017.

References

1. Chitnis A, Balle-Cuif L. The Notch meeting: an odyssey from structure to function. Development 2016;143:547–53.
2. Andersson ER, Lendahl U. Therapeutic modulation of Notch signalling–are we there yet? Nat Rev Drug Discov 2014;13:357–78.
3. Ntziachristos P, Lim JS, Sage J, Aifantis I. From fly wings to targeted cancer therapies: a centennial for notch signaling. Cancer Cell 2014;25:318–34.
4. Takebe N, Miele L, Harris PJ, Jeong W, Bando H, Kahn M, et al. Targeting Notch, Hedgehog, and Wnt pathways in cancer stem cells: clinical update. Nat Rev Clin Oncol 2015;12:445–64.
5. Kreso A, Dick JE. Evolution of the cancer stem cell model. Cell Stem Cell 2014;14:275–91.
6. Visvader JE, Lindeman GJ. Cancer stem cells: current status and evolving complexities. Cell Stem Cell 2012;10:717–28.
7. Li Y, Rogoff HA, Keates S, Gao Y, Murikipudi S, Mikule K, et al. Suppression of cancer relapse and metastasis by inhibiting cancer stemness. Proc Natl Acad Sci U S A 2015;112:1839–44.
8. Reya T, Morrison SJ, Clarke MF, Weissman IL. Stem cells, cancer, and cancer stem cells. Nature 2001;414:105–11.

9. Colak S, Medema JP. Cancer stem cells–important players in tumor therapy resistance. FEBS J 2014;281:4779–91.
10. Sun S, Liu S, Duan SZ, Zhang L, Zhou H, Hu Y, et al. Targeting the c-Met/FZD8 signaling axis eliminates patient-derived cancer stem-like cells in head and neck squamous carcinomas. Cancer Res 2014;74:7546–59.
11. Pattabiraman DR, Weinberg RA. Tackling the cancer stem cells - what challenges do they pose? Nat Rev Drug Discov 2014;13:497–512.
12. Marcucci F, Rumio C, Lefoulon F. Anti-cancer stem-like cell compounds in clinical development - an overview and critical appraisal. Front Oncol 2016;6:115.
13. Samon JB, Castillo-Martin M, Hadler M, Ambesi-Impiobato A, Paietta E, Racevskis J, et al. Preclinical analysis of the gamma-secretase inhibitor PF-03084014 in combination with glucocorticoids in T-cell acute lymphoblastic leukemia. Mol Cancer Ther 2012;11:1565–75.
14. Wang K, Zhang Q, Li D, Ching K, Zhang C, Zheng X, et al. PEST domain mutations in Notch receptors comprise an oncogenic driver segment in triple-negative breast cancer sensitive to a gamma-secretase inhibitor. Clin Cancer Res 2015;21:1487–96.
15. Zhang CC, Pavlicek A, Zhang Q, Lira ME, Painter CL, Yan Z, et al. Biomarker and pharmacologic evaluation of the gamma-secretase inhibitor PF-03084014 in breast cancer models. Clin Cancer Res 2012;18:5008–19.
16. Yabuuchi S, Pai SG, Campbell NR, de Wilde RF, De Oliveira E, Korangath P, et al. Notch signaling pathway targeted therapy suppresses tumor progression and metastatic spread in pancreatic cancer. Cancer Lett 2013;335:41–51.
17. Cui D, Dai J, Keller JM, Mizokami A, Xia S, Keller ET. Notch pathway inhibition using PF-03084014, a gamma-secretase inhibitor (GSI), enhances the antitumor effect of docetaxel in prostate cancer. Clin Cancer Res 2015;21:4619–29.
18. Arcaroli JJ, Quackenbush KS, Purkey A, Powell RW, Pitts TM, Bagby S, et al. Tumours with elevated levels of the Notch and Wnt pathways exhibit efficacy to PF-03084014, a gamma-secretase inhibitor, in a preclinical colorectal explant model. Br J Cancer 2013;109:667–75.
19. Banerjee D, Hernandez SL, Garcia A, Kangsamaksin T, Sbiroli E, Andrews J, et al. Notch suppresses angiogenesis and progression of hepatic metastases. Cancer Res 2015;75:1592–602.
20. Papayannidis C, DeAngelo DJ, Stock W, Huang B, Shaik MN, Cesari R, et al. A Phase 1 study of the novel gamma-secretase inhibitor PF-03084014 in patients with T-cell acute lymphoblastic leukemia and T-cell lymphoblastic lymphoma. Blood Cancer J 2015;5:e350.
21. Hughes DP, Kummar S, Lazar AJ. New, tolerable gamma-secretase inhibitor takes desmoid down a notch. Clin Cancer Res 2015;21:7–9.
22. Wang XQ, Zhang W, Lui EL, Zhu Y, Lu P, Yu X, et al. Notch1-Snail1-E-cadherin pathway in metastatic hepatocellular carcinoma. Int J Cancer 2012;131:E163–72.
23. Tang ZY, Ye SL, Liu YK, Qin LX, Sun HC, Ye QH, et al. A decade's studies on metastasis of hepatocellular carcinoma. J Cancer Res Clin Oncol 2004;130:187–96.
24. Rubio-Viqueira B, Jimeno A, Cusatis G, Zhang X, Iacobuzio-Donahue C, Karikari C, et al. An *in vivo* platform for translational drug development in pancreatic cancer. Clin Cancer Res 2006;12:4652–61.
25. Hermann PC, Huber SL, Herrler T, Aicher A, Ellwart JW, Guba M, et al. Distinct populations of cancer stem cells determine tumor growth and metastatic activity in human pancreatic cancer. Cell Stem Cell 2007;1:313–23.
26. Yamashita T, Honda M, Nakamoto Y, Baba M, Nio K, Hara Y, et al. Discrete nature of EpCAM+ and CD90+ cancer stem cells in human hepatocellular carcinoma. Hepatology 2013;57:1484–97.
27. Menendez JA, Joven J, Cufi S, Corominas-Faja B, Oliveras-Ferraros C, Cuyas E, et al. The Warburg effect version 2.0: metabolic reprogramming of cancer stem cells. Cell Cycle 2013;12:1166–79.
28. Steeg PS. Targeting metastasis. Nat Rev Cancer 2016;16:201–18.
29. Tung-Ping Poon R, Fan ST, Wong J. Risk factors, prevention, and management of postoperative recurrence after resection of hepatocellular carcinoma. Ann Surg 2000;232:10–24.
30. Blaskovich MA, Sun J, Cantor A, Turkson J, Jove R, Sebti SM. Discovery of JSI-124 (cucurbitacin I), a selective Janus kinase/signal transducer and activator of transcription 3 signaling pathway inhibitor with potent antitumor activity against human and murine cancer cells in mice. Cancer Res 2003;63:1270–9.
31. Liu L, McBride KM, Reich NC. STAT3 nuclear import is independent of tyrosine phosphorylation and mediated by importin-alpha3. Proc Natl Acad Sci U S A 2005;102:8150–5.
32. Wang XQ, Lo CM, Chen L, Ngan ES, Xu A, Poon RY. CDK1-PDK1-PI3K/Akt signaling pathway regulates embryonic and induced pluripotency. Cell Death Differ 2017;24:48–48.
33. Buettner R, Mora LB, Jove R. Activated STAT signaling in human tumors provides novel molecular targets for therapeutic intervention. Clin Cancer Res 2002;8:945–54.
34. Bowman T, Garcia R, Turkson J, Jove R. STATs in oncogenesis. Oncogene 2000;19:2474–88.
35. Darnell JE. Validating Stat3 in cancer therapy. Nat Med 2005;11:595–6.
36. Geisler F, Strazzabosco M. Emerging roles of Notch signaling in liver disease. Hepatology 2015;61:382–92.
37. Morell CM, Strazzabosco M. Notch signaling and new therapeutic options in liver disease. J Hepatol 2014;60:885–90.
38. Villanueva A, Alsinet C, Yanger K, Hoshida Y, Zong Y, Toffanin S, et al. Notch signaling is activated in human hepatocellular carcinoma and induces tumor formation in mice. Gastroenterology 2012;143:1660–9.
39. Nishida N, Kitano M, Sakurai T, Kudo M. Molecular mechanism and prediction of sorafenib chemoresistance in human hepatocellular carcinoma. Dig Dis 2015;33:771–9.
40. Androutsellis-Theotokis A, Leker RR, Soldner F, Hoeppner DJ, Ravin R, Poser SW, et al. Notch signalling regulates stem cell numbers *in vitro* and *in vivo*. Nature 2006;442:823–6.